International Journal of Extreme Manufacturing

TOPICAL REVIEW • OPEN ACCESS

A review on glass welding by ultra-short laser pulses

OPEN ACCESS
IOP Publishing | IMMT
International Journal of Extreme Manufacturing
Int. J. Extrem. Manuf. 1 (2019) 042001 (10pp)
https://doi.org/10.1088/2631-7990/ab55f6

Topical Review

A review on glass welding by ultra-short laser pulses

Kristian Cvecek[1,2], Sarah Dehmel[3], Isamu Miyamoto[2,4] and Michael Schmidt[1,2,3]

[1] Institute of Photonic Technologies, Friedrich-Alexander-Universität Erlangen-Nürnberg, Erlangen, Germany
[2] SAOT—Erlangen Graduate School in Advanced Optical Technologies, Friedrich-Alexander-Universität Erlangen-Nürnberg, Erlangen, Germany
[3] blz—Bayerisches Laserzentrum GmbH, Erlangen, Germany
[4] Osaka University, Osaka, Japan

E-mail: kristian.cvecek@lpt.uni-erlangen.de

Received 6 October 2019, revised 8 November 2019
Accepted for publication 11 November 2019
Published 16 December 2019

Abstract

Glass welding by ultra-short pulsed (USP) lasers is a piece of technology that offers high strength joints with hermetic sealing. The joints are typically formed in glass that is transparent to the laser by exploiting nonlinear absorption effects that occur under extreme conditions. Though the temperature reached during the process is on the order of a few 1000 °C, the heat affected zone (HAZ) is confined to only tens of micrometers. It is this controlled confinement of the HAZ during the joining process that makes this technology so appealing to a multitude of applications because it allows the foregoing of a subsequent tempering step that is typically essential in other glass joining techniques, thus making it possible to effectively join highly heat sensitive components. In this work, we give an overview on the process, development and applications of glass welding by USP lasers.

Keywords: USP glass welding, ultra-short pulsed laser processing, brittle materials, glass joining

1. Introduction

The usage of glass in most industrial or technical applications is motivated by its compelling physical properties, such as low absorptivity (down to 0.2 dB km^{-1} [1]), high chemical inertness [2, 3] and high melting points (e.g. 1710 °C softening point for fused silica [4]). Glass is also the material of choice for tasks requiring a tailored refractive index, which can be efficiently achieved by mixing dopant atoms into the SiO_2 glass matrix. Additionally, glass is essentially refined sand—an abundant resource on Earth [5], and thus, is both economical and easily accessible.

However, for real-world applications, simple 'blocks' of glass do not offer enough functionality. Glass often requires some assembly or joining to provide practical functionality. The above-mentioned desirable characteristics of glass, including low absorptivity, high chemical stability, and high melting points, unfortunately increase the complexity of joining. Though established technologies for glass joining do exist, these technologies have certain limitations so that in choosing a suitable joining technology, the specific use case of the final component needs to be considered.

As an example, while mechanical mounting [6], gluing [7] and soldering [8] are fairly straightforward glass joining techniques, they are not optimal when additional (and thus different) materials are present in the joint, which causes a mismatch of thermal expansion coefficients and reduced chemical stability. This deficiency is not present when no additives are used. Such is the case in optical contacting [9] also, though it is, however,

susceptible to impact loads [10]. Last but not least, thermal diffusion bonding [11] and CO_2-laser welding [12] are both effective glass joining techniques as well, but both are relatively slow processes since the components that are to be joined need to be exposed to high temperatures for hours.

With the availability of ultra-short pulsed (USP) lasers with both sufficiently high pulse energy and repetition rate, an additional glass joining process has become available in the last decade. This process, glass welding by USP lasers (abbreviated as 'USP glass welding'), not only does not require additional materials or long processing times, but also offers the benefit of true fusion welding of glass components.

The structure of this paper is as follows: in section 2, a brief historical overview will be given on the initial development of the process. Section 3 will discuss the underlying physics, and section 4 will explore novel developments and applications.

2. Development of USP based glass welding

A first description of USP glass welding was documented by Tamaki *et al* [13] in 2005. Interestingly, this research group has already filed a patent on this technology in 2003 [14]. The welding parameters used by Tamaki *et al* at that time were a feed speed of 5 μm s^{-1} at a repetition rate of 1 kHz, using pulses with 130 fs FWHM pulse duration at 800 nm. While nowadays, much higher feed speeds and repetition rates are typically used, those parameters might have been due to the lack of availability of high repetition USP laser sources. Nevertheless, by 2005, research on glass welding by USP lasers was on the rise, as evident by another patent being filed on this technology by in 2005 IMRA America Inc. [15] and an additional publication by Tamaki *et al* in 2006 [16].

All the published research thus far has implemented femtosecond pulsed lasers. Unfortunately, these laser sources were not yet suitable for implementation in a 24/7 industrial production environment due to issues in long-term stability and maintenance. In contrast, picosecond pulsed laser systems were already considered for industrial applications, as is evidenced by the first implementation of picosecond pulsed lasers in serial production by Bosch in 2007 [17, 18]. Prompted by these developments and improvements in laser sources [19], the USP glass welding process was demonstrated to also work with pulses of 10 ps duration in 2007 [20]. Since then, the breadth and depth of the ongoing research on USP glass welding has incorporated a multitude of glass and material types, as well as a variety of beam focusing configurations and irradiation strategies, which will be discussed in greater detail in section 4.

3. Underlying physics

3.1. Basic principles

A schematic drawing of the USP glass welding process is shown in figure 1 along with an example technical implementation. The conditions for the experimental implementation of relevant figures are given in table 1 at the end of section 4. The sample is either moved with regards to the laser or a scanner is used to deflect the beam. The choice primarily depends on the requirements the welding must fulfill. The focusing objective typically has a relatively high numerical aperture (NA) on the order of ca. 0.4, in order to keep the melt pool localized, which is important in reducing the crack tendency (compare section 3.2). Nevertheless, the process has also been demonstrated for much lower NAs (see section 4.3).

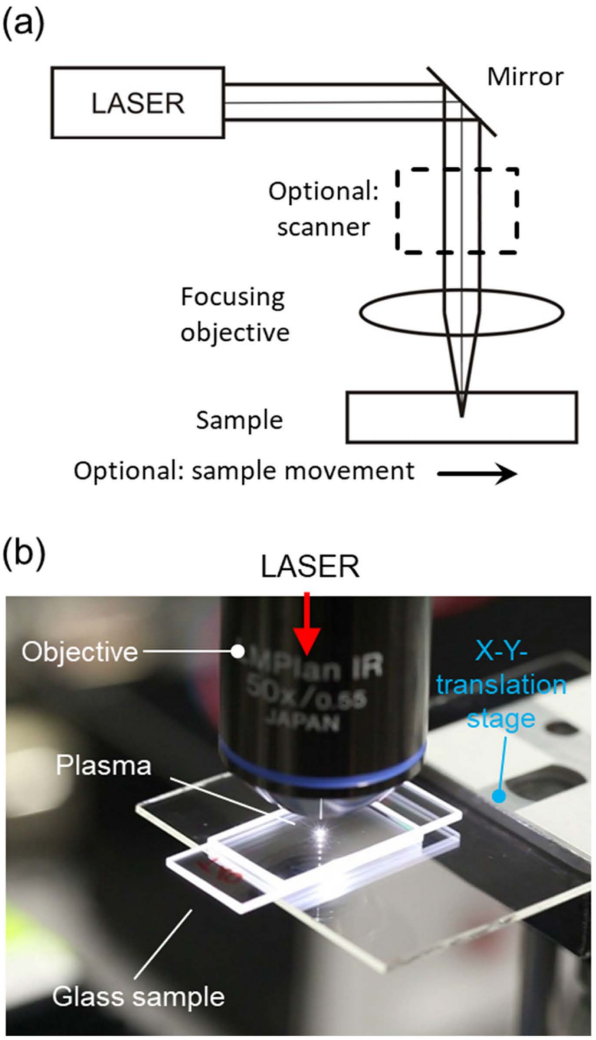

Figure 1. Schematic setup of USP glass welding (a) and an example technical implementation (b). See table 1 for experimental conditions.

In USP glass welding, lasers are used that have a wavelength to which the glass is transparent. The energy input is established via nonlinear absorption [21, 22] (e.g multi photon ionization), i.e. when the laser intensity reaches sufficiently high values. Depending on the properties of both the focusing optics and pulse duration, self-focusing effects may influence the shape of the focal spot generating the free

Table 1. Summary of used experimental conditions in figures 1, 3, 4, 5 and 7. The laser wavelength was in all cases 1064 nm and the FWHM pulse duration 10 ps. NA stand for the numerical aperture of the focusing objective, ω is the focal spot radius, P is the average laser power, v is the feed speed, f is the pulse repetition frequency, Δz is the displacement from the reference surface 'rs', where USLG stands for 'upper surface of lower glass plate' and US stands for 'upper surface' of a single glass plate.

Figure	NA	ω (μm)	P (W)	v (mm s^{-1})	f (MHz)	Δz (μm)	rs
1(b)	0.55	1.5	2	20	1	−20	USLG
3	0.55	1.5	6	20	0.1	−200	US
4(a)	0.55	1.5	6	50	8.2	−150	US
4(b)	0.55	1.5	5	20	1	−150	US
5	0.55	1.5	2.3	20	1	−200	US
7	0.8	0.9	6	200	1	−150	US

electrons [23]. However, the self-focusing effects can be minimized by using low enough pulse energies or high enough focusing NAs [24]. The multiphoton ionization can be accompanied by avalanche ionization as well [25] (within the same pulse) if the pulse is long enough [26]. The addition of avalanche ionization can dramatically increase the free electron density and thereby further raise the absorptivity of the irradiated region.

The generated free electrons will subsequently transfer their kinetic energy to the glass lattice and heat the glass material. If the next pulse arrives 'early' and overlaps enough with the first pulse (by choosing a suitable pulse repetition rate and feed speed) such that the temperature of the glass has not returned to room temperature, the heat will accumulate (illustrated figure 2) close to the focal region with each incoming pulse [27] until a quasi-static state is reached. The highest achievable temperatures can lie in the range of few thousand °C [27], where thermal ionization also takes place.

Since plasma, i.e. free electrons, is typically an outstanding absorber [28, 29], the ionization process can take place far above the actual focus position, as seen in figure 3 (compare [30]) and as demonstrated by simulations in [27]. Even at comparably low temperatures (several hundred °C), thermal ionization is critical, since even when only a few free electrons are generated by thermal ionization, they can contribute significantly to the avalanche ionization process [31]. As can be seen from figure 2(a), the glass will not reach the same temperature as further upstream along the focus. The reason for this is that plasma absorbs most of the laser energy further 'upstream' and causes partial shielding of the laser beam. This lower effective absorptivity and smaller temperatures are the reason for the development of the tear drop shape of the molten zone.

As illustrated in figure 3, the time-dependent plasma generation takes place predominantly 'upstream' of the laser beam direction because the already-generated plasma will have a shielding effect on the irradiation at the position of the nominal geometric focal spot [32]. However, the instability of this situation results in quasi-periodic plasma motion, where plasma generated in the focal spot moves toward the incoming laser beam (compare the supplementary material in [33]). This effect has been confirmed by other experiments and simulations as well [30, 34].

The typical shape of the laser modified glass is shown in figure 4 for fused silica and D263 glass. As displayed, the

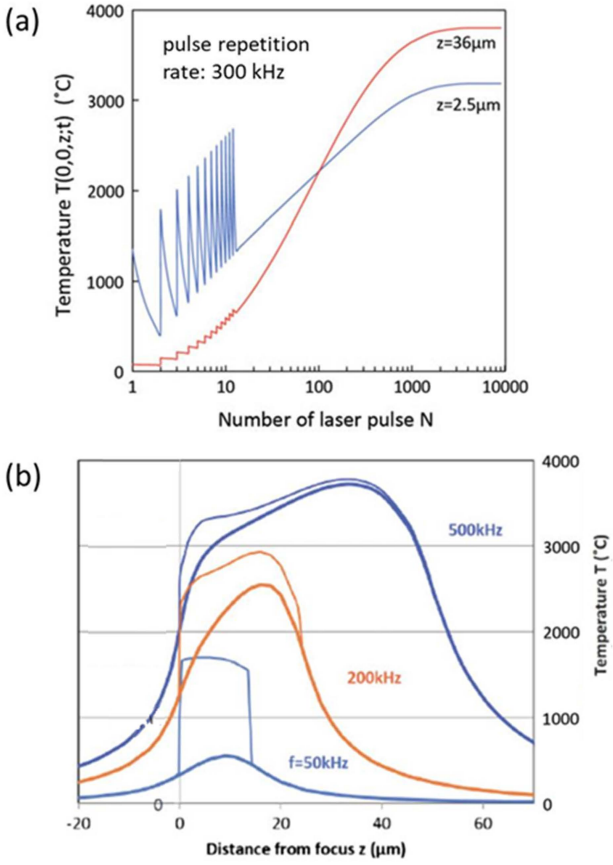

Figure 2. Empirical fit of temporal temperature development on experimental data, see [27] for details. The temperature development along the optical axis for different distances z from the focal spot (a) with regards to the number of applied pulses (a) and the temperature distribution along the optical axis ($z = 0$ is the focal spot) for the steady state case (b). [27] © Springer-Verlag Berlin Heidelberg 2013. With permission of Springer.

cross-section of the laser modified zone is teardrop shaped for both glass types. The tendency to form a teardrop shape is already visible in figure 3. The teardrop shape is actually caused by a time-average of the laser absorption during the highly dynamic plasma behavior mentioned above. Evidently, as demonstrated by the temperature distribution in figure 2, on average, most of the input laser power is absorbed far above the focal point. In turn, the time-averaged portion of laser power that still reaches the focal spot is significantly smaller

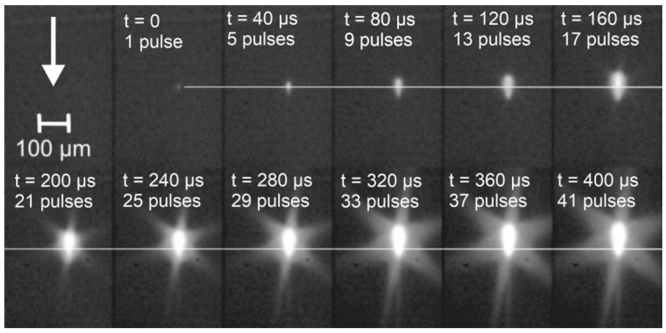

Figure 3. Temporal development of plasma in glass during USP glass welding across 0.4 ms. The nominal focus position is indicated by the white line. The laser beam propagation direction is indicated by the white arrow. For further details, see [30]. See table 1 for experimental conditions. (The motion of the stage of 8 μm for the total duration of the shown image series cannot be resolved.) Reprinted from [30], © 2018 Published by Elsevier B.V. with permission from Elsevier.

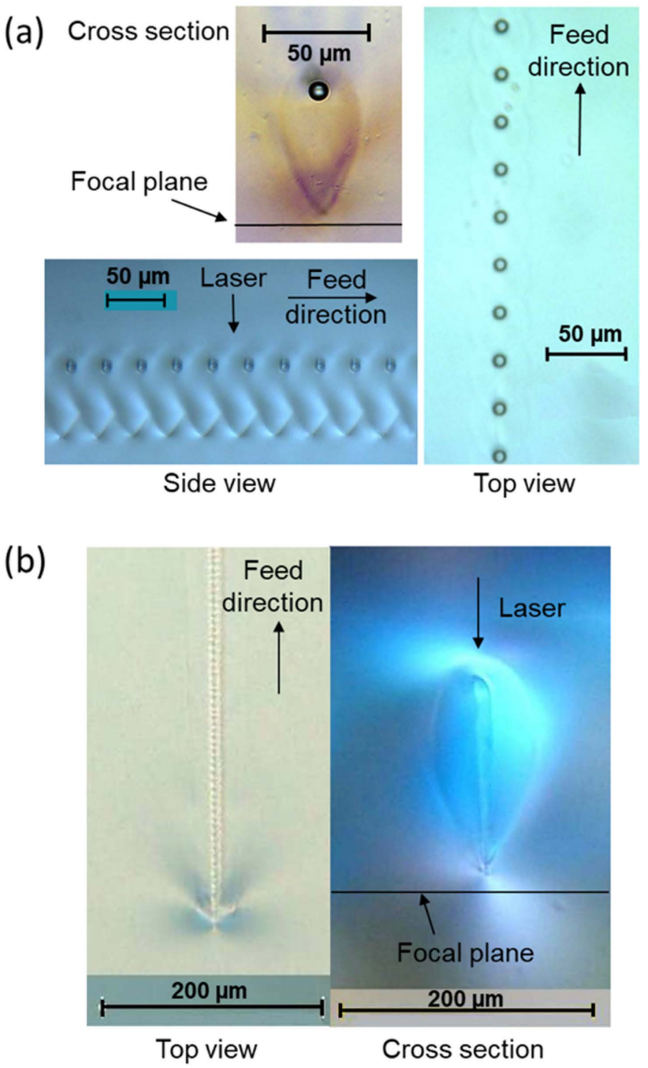

Figure 4. Typical shape of laser modified glass for fused silica (a) and D263 borosilicate glass (b). See table 1 for experimental conditions.

and therefore, is often not high enough to precipitate the formation of the rounded tip of the tear drop. Nevertheless, the actual shape of the melt pool depends on factors such as the numerical aperture of the focusing optics as well as the feed speed, average laser power, heat conductivity, and melting point of the glass material in question. Thus, both elliptical and circular cross sections can be achieved [34, 35]. Shape is important when considering defect formation mechanisms during USP glass welding, which will be discussed in section 3.2.

The reasons behind the appearance of the laser modified zone or, in other words, the melt pool, are not yet fully comprehended, since the laser modified area is only visible through the changes in its refractive index during optical microscope observation. In addition to USP glass welding, waveguide writing [36] and selective laser etching [37] utilize laser induced modifications. In order to further develop and improve the USP glass welding process, it is essential to thoroughly understand the underlying processes.

Thus far, on one hand, there is the difference between the inner structure within the modified zone of the D263 glass (figure 4(b)) and the fused silica (figure 4(a)). The inner structure of the D263 glass (and also in other glass types) corresponds to the location of the plasma region, in which the oxygen gas bubbles (often called voids in literature on USP glass welding) in fused silica are also confined [38, 39]; compare figure 4(a). This observed behavior can be explained by space-selective phase separation [40].

On the other hand, the viscosity of most glass types depends on temperature [41] and since the temperature distribution during the process should be continuous as well, it is quite extraordinary to observe the discontinuous refractive index changes that gave rise to the boundaries of the laser modified zones in figure 4. So far, the temperatures corresponding to this boundary are being attributed to the working point of the glass with a viscosity of ca. 10^4 Pa s and remain at 1051 °C for D263 glass [27]. Direct temperature measurements, e.g. by Raman spectroscopy [42], are challenging to conduct during irradiation due to the strong and broadband black body radiation of a material in a temperature range of several 1000 K (compare figure 2, [27] and [42]).

Despite these high temperatures, USP glass welding allows the joining of glass pieces with temperature sensitive components, such as electronics or organics, e.g. for lab-on-chip applications. This is possible because the melt pool boundary (as described above), which has a temperature that reaches the working point of the glass, has dimensions up to only a few hundred micrometers (compare figure 2). The resulting steep temperature gradients prompt a fast cooling and efficient heat dissipation. Thus, glass in the vicinity of a few millimeters will remain at the ambient (room) temperature. This is corroborated by a thermographic image illustrated in figure 5, displaying a fused silica glass sample. As can be seen, the range of the area of glass that is 5 K above room temperature is strongly localized. Of course, temperature sensitive components must not be placed directly on the path of the welding seam.

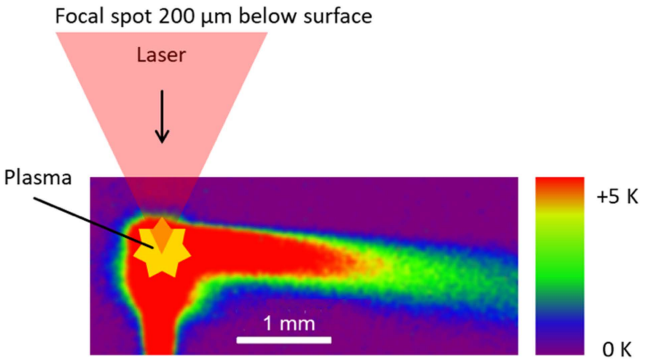

Figure 5. Thermographic image of the USP glass welding process in fused silica. See table 1 for experimental conditions.

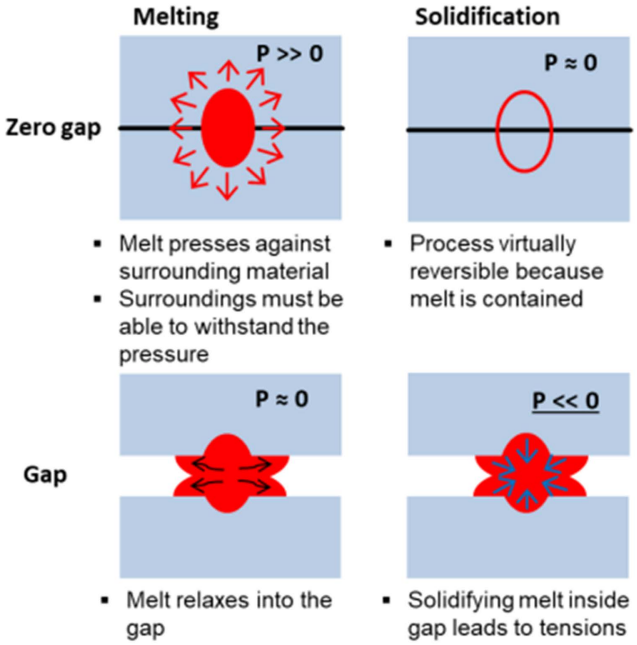

Figure 6. Schematic comparison between zero-gap and gap welding from which the cracking tendency of USP welding seams can be inferred.

3.2. Crack formation prevention

The aforementioned strong localization of the melt pool during the USP glass welding process is also essential to achieving high strength joints. A detailed explanation can be found in [27, 43], but is briefly described here.

For simplification purposes we assume here that the glass will not change its crystallographic state during (e.g. increasing its volume) when undergoing the relatively rapid quenching in a typical USP glass welding process [44]. Consider now figure 6 in which two scenarios with a liquid melt pool are displayed. One illustrates a zero-gap welding, while the other demonstrates a gap in the welding. During the heat-up, e.g. when the laser is absorbed by the material, the melt pool forms and thermal expansion occurs. In the zero-gap-situation, large compressive stresses will occur. Depending on the magnitude of these stresses, the plates may be pushed apart or the surrounding glass material may get damaged. But for the time being, let us assume that the stresses are not too large due to the melt pool being small enough that the compressive stresses do not damage the glass or push the samples apart.

In contrast, in the situation with the gap present, the liquid melt will have a free surface that can relax into the gap. Hence, there will be minimal compressive stresses during the heat-up, even though thermal expansion will take place. After heat-up, cooldown will naturally follow. For glass in a temperature range between 1000 °C and 2000 °C, the cooldown process is dominated by heat conduction over radiative losses. (This can easily be proven by comparing the heat flux from a small spherical region at temperature T, with a radius smaller than 100 μm, to approximately infinity in glass with radiated power loss from same region, as described by the Stefan–Boltzmann law.) Therefore, the melt will solidify from outside to inside (in both cases). In the zero-gap-scenario, the compressive stresses will diminish due to thermal shrinkage. Ultimately, the resolidified material will experience approximately the same amount of stress as before the welding process. In comparison, the melt, which was able to relax the compressive stresses into the gap, will experience tensile stresses after resolidification. These tensile stresses will be approximately the same magnitude (but inverse sign) as the compressive stresses in the zero-gap scenario (when disregarding the slight irreversibility of the glass's volume expansion during cooldown). However, glass are usually about 20 times more resilient against compressive stresses than against tensile stresses [45]. Hence, in theory, damage-free welding with a melt pool that is twenty times larger should be feasible in the zero-gap scenario. Moreover, if a gap exists during welding, residual tensile stresses will be present in the welded specimen, unless it is post-processed by heat treatment (as is typically the case for CO_2-laser welded glass samples).

This is why initial efforts were made to reduce the gap as much as possible, be it by outside mechanical pressure [16] or by optical contacting [46, 47]. Additionally, special attention must be paid to the density of the welding seams, since welding seam density that is too high will lead to the accumulation of residual stresses due to irreversible volume expansion from rapid quenching, which will in turn decrease the stability of the weld seam, as demonstrated by experiments conducted in [47]. Optical contacting has been adopted by several research groups, since it can provide least residual stresses in the welded specimen, but is, unfortunately, not currently readily available for industrial applications. This is because typical values necessary for optical contact of two plane plates are <0.5 nm in surface roughness, <5 μm in total thickness variation, and <30 μm in flatness [48]. Though it is possible to achieve optical contact with lower surface quality, the optical contact achieved may not cover the entire area of the plates. Thus, it is necessary to find glass joining methods that achieves both the ability to circumvent the crack formation inside the gap and the ability to bridge the gap. The research conducted on this topic will be discussed in section 4.1.

Nonetheless, crack formation due to melt relaxation into the gap is not the only type of defect that occurs during USP glass welding. For instance, if too much laser power is used, the bulk material might not be able to withstand the compressive stresses during irradiation [49]. Another scenario with a high potential of crack formation occurs at the start of the welding process, when nonlinear absorption is taking place within the still cold, and thus brittle, glass material [50]. Depending on the size of these initial cracks, the laser pulse energy, and the feed speed, the subsequent melt formation can, in principle, 'overtake' the cracks, i.e. the glass area where the cracks have propagated into can become combined with the growing melt pool. As soon as the plasma region is enclosed by a melt pool, no further cracks will form, let alone propagate outside the melt pool.

This is unfortunately valid as long as the shape of the molten pool, i.e. the aspect ratio of its cross-section, is sufficiently close to 1:1. If the deviation becomes too large, then the melt pool may begin to act as a wedge, thereby creating cracks in the material. If taken to extremes, a very high aspect ratio can be used for USP glass cutting [51]. To prevent this from happening during USP glass welding, focusing optics with rather large numerical apertures should be used.

Besides crack formation, gas bubble formation can also be observed in certain glass types, such as fused silica (see figure 4(a) [38]). Depending on the processing parameters, the gas bubbles can grow to such a significant size that the continuous generation of plasma will be interrupted, thus spontaneously disrupting the heating process, resulting in a local but significantly reduced size of the welding seam [38], as illustrated in figure 7.

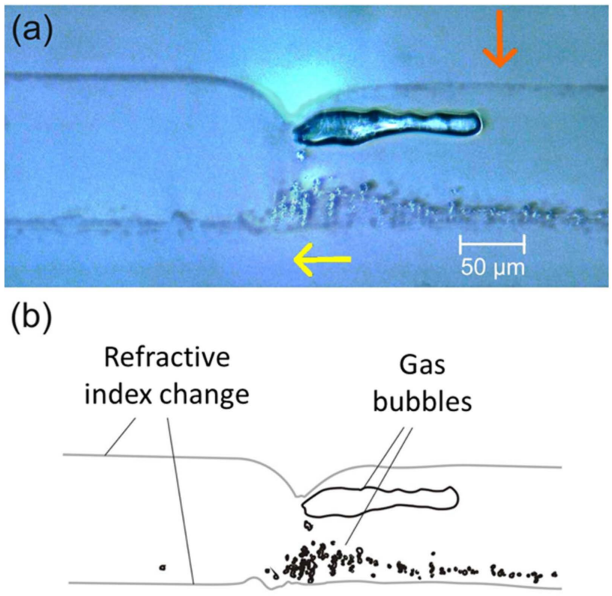

Figure 7. Microscope photograph, side view, of a gas bubble formed in fused silica, observed under crossed polarizers. The red arrow depicts the incoming laser direction, and the yellow arrow shows the feed direction of the sample. See [38] for further details. See table 1 for experimental conditions.

3.3. Numerical simulations

Any model that intends to simulate the USP glass welding processes must consider not only the initial absorption of the laser pulses by nonlinear effects, but also the subsequent interactions and effects, including avalanche ionization, thermal ionization, as well as the heat conduction and dissipation phenomena, over the course of at least several hundred pulses, or better yet, several thousand pulses. This necessitates a mathematical description of the effects from ultra-short time scales, as well as time scales that range up to milliseconds or seconds. Moreover, a good simulation needs to include how the properties of the material evolve in a range of temperatures, from room temperature to up to several thousand degrees, such that all possible phase state transitions among solid, fluid, gaseous and plasma states, would be considered. There are also other processes and effects that may be important to consider, such as transient laser beam distortions due to thermal lensing, as well as refraction and scattering on the plasma, or various chemical processes taking place inside the hot glass melt (or plasma), which can lead to phase separation or changes in the crystallographic structures. The incorporation of all pertinent effects (of which so far only a non-exhaustive list has been given) into a simulation would require an enormous effort and running the simulation would be very time intensive. Therefore, due to time and resource constraints, the simulation must concentrate on pertinent aspects that arise from the proposed theories and hypotheses, which are typically tested in parallel by multiple experiments.

Most research around the simulation of USP glass welding has thus been limited to simulating the glass welding process through reducing the problem to nonlinear absorption, which is described by the Keldysh model and multi-photon ionization [52], followed by avalanche [26] and thermal ionization [31]. The energy input into the plasma is then considered to be a heat source that heats the glass material. Through the relationship between temperature and plasma-density/laser-pulse-energy, the absorbed energy and heat distribution can be established [34]. Subsequently, the laser-pulse/glass interaction heat diffusion will be considered, from which the time-dependent temperature distribution can be calculated [34]. In order to consider the effect of thermally excited electrons, the residual electron density prior to an incoming laser pulse is calculated from the temperature distribution, using both Boltzmann statistics and the band-gap energy of the glass in question. Thus far, only a rudimentary description has been provided, along with citations of simulations employing the discussed methodologies; however, in practice, effects can be incorporated into a simulation in a variety of ways, depending on how much fundamental or empirical backing of the simulation is desired or necessary. Unfortunately, a comprehensive description of simulation research on USP glass welding is not in scope for the research described in this paper. Nonetheless, following publications are cited [26, 27, 31, 34, 52, 53] and the literature therein will provide further details.

In table 1, a summary of the experimental conditions for figures 1, 3, 4, 5 and 7 is given.

4. Further developments and applications

4.1. Gap bridging

As previously mentioned in section 3.2, the crack formation tendency is increased when USP glass welding is conducted inside a gap. One possible approach to preventing crack formation is employing outside clamping to reduce gap size [16]. However, it is likely that the sample will experience residual stresses after welding as soon as the clamping device is removed since the joining partners may bend into the welding position. Optical contacting can circumvent these problems but unfortunately, cannot be readily automated for industrial applications.

Therefore, gap bridging methods for USP glass welding have attracted the attention of researchers and have been thoroughly investigated. In 2015, the first successful experimental results were published by three independent research groups [44, 54, 55]. The experiment of one of the authors of this paper [44] was based on the hypothesis that the glass surrounding the plasma zone will have a distribution of viscosities at which the glass is still moldable, due to temperature distribution (refer to figure 2(b) or [27]). If this moldable zone occurs close enough to the surface of the glass plate, then the surface should bulge outwards without cracking. In order to prevent uncontrolled melt relaxation into the gap, the surface temperature should be low enough to cause sufficiently high surface tension (refer to the Eötvös rule [56]). A type of irreversible bulging occurring within a smooth surface was indeed confirmed in [44], thus implying the possibility of reversible bulging with larger amplitudes in the presence of a transient thermal expansion of the melt pool. In the event that this bulge closes a gap to a second glass plate, van der Waals forces should provide initial direct contact and bonding forces, while heat conduction should lead to a softening of the other joining partner's surface. During cooldown, the shrinkage of the molten pool should attract both joining partners to each other via van der Waals forces, thereby reducing the gap. A subsequent welding seam at a new position might benefit from the partially reduced gap and thus provide improved bonding and stronger gap reduction. At some point, even molecular diffusion might be possible since the observed bonding energies exceed the bonding energy of pure van der Waals bonding, i.e. optical contact, by a large margin. Gap bridging was found to be effective for soda-lime/soda-lime glass, BOROFLOAT33/BOROFLOAT33 and D263/D263 borosilicate glass, as well as fused-silica/fused-silica. The bridgeable gap was found to be up to 1 μm at a pulse energy of 2 μJ, a pulse repetition rate of 1 MHz, and a FWHM pulse duration of 10 ps.

The research experiments in [54] were conducted for BOROFLOAT33/N-BK7 glass and fused-silica/fused-silica. The experiments were focused on the focal spot position and the dependency of successful gap bridging on pulse energy. The results support the hypothesis that the melt pool should be concentrated within approximately one welding partner, which allows the processing parameter window to be larger. It was also shown that for high enough pulse energies, bridging can take place even when the melt pool is centered on the gap. The achieved bridgeable gap was about 3 μm at a pulse energy of 18.4 μJ, a pulse repetition rate of 400 kHz, and an FHWM pulse duration of 5.9 ps. Remarkably, a linear dependency of the bridgeable gap size on the laser pulse energy was discovered. Overall, the findings of [54] suggest that the hypothesis of [44] is incomplete since the surface tension of a centrally positioned, but sufficiently large, melt pool can still be high enough to prevent melt relaxation into the gap. Nevertheless, these results suggest the existence of an upper limit to the crack-free bridgeable gap size as well, because when the melt pool becomes too large, even in bulk material, cracks will form around the resolidified melt pool, as referenced in [49]. One of the glass materials tested at high pulse energies in [54], fused-silica/fused-silica, has a very low thermal expansion coefficient and thus exhibits an extremely favorable behavior for bridging large gaps.

In [55], fused-silica/fused-silica gap bridging was examined using pulse bursts of four pulses at 10 μJ (20 ns inter-burst period), with a FWHM pulse duration of 0.5 ps at 200 kHz burst repetition rate. The maximum bridged gap was about 3 μm. In terms of absorbed laser power, the experiment in [55] is similar to [54] because under a heat accumulation regime, the nonlinearly absorbed energy is governed by an interaction of thermal ionization with avalanche ionization, and is thus relatively independent of the peak intensities achieved in the focal spot (which have a large impact on the initial absorptivity of the USP glass welding process). Depending on the temperatures reached in the welding seam, the absorptivity lies typically between 60 and 90%, independent of the pulse repetition rate or pulse duration [27, 54]. Hence, in terms of absorbed power, [55] is roughly comparable to [54], thereby confirming the results of [54].

Recently, a novel gap bridging mechanism has demonstrated the ability to bridge gaps of about 10 μm by using a small-scale rapid oscillating scan at a very low numerical aperture [57] in soda-lime/soda-lime glass. The FWHM pulse duration was 10 ps at 1 MHz pulse repetition rate and 12 μJ pulse energy. A galvanometer scanner with a focusing lens of 103 mm (20 μm focal spot diameter) was used to inscribe concentrically hatched circles with radii of 300 μm. In order to achieve heat accumulation, the beam deflection speed was set to 1 m s^{-1}, while the structure was irradiated sequentially 150 times. The resulting (relatively large) molten pool was able to reduce the gap between the glass plates down to ca. 3 μm. However, cracks were present inside the welding area. This could be due to several factors, one being the extremely large melt pool when compared to the typically high NA USP glass welding, the other being that soda-lime glass has a very high thermal expansion coefficient when compared to fused silica (approx. 90 $\times$ 10^{-7} 1/K [58] versus 5–6 $\times$ 10^{-7} [59]). The authors of [57] reported an achieved breaking strength of around 65 MPa (no Weibull statistics conducted) while [55] reported a ca. 73 MPa breaking strength for 63.2% failure probability, determined from Weibull evaluation.

4.2. Multi-material joining

So far, only the most prominent issues of USP glass welding have been addressed. However, for industrial applications, the joining of dissimilar materials is often necessary in fulfilling a wide array of demands imposed by the intended application area. Logically, in the initial stages of an experiment, typically the same-glass materials are used for both joining partners. USP glass welding has been proven to be able to join a multitude of same-glass combinations with glass types such as soda-lime [44, 57], borosilicate glasses (e.g. BOROFLOAT33 [44, 46], D263 [44, 46, 60], N-BK7 [61]), fused-silica [13, 44, 47, 54, 55, 60] and FOTURAN [62, 63] (of course, neither the list of glass types nor the list of citations are exhaustive).

In addition USP glass welding of same-glass combinations, many research studies have also been conducted on the combinations of various types of glass, such as N-BK7 to BOROFLOAT33 [54], fused-silica to BK7 [64], or fused-silica to borosilicate HOYA NA35 [65]. Evidently, even if dissimilar glass types are used as joining partners, the process preconditions are still similar to same-glass joining. However, this changes dramatically if one of the joining partners is a non-transparent or non-vitreous material (due to a discontinuous viscosity dependence on temperature).

The USP laser joining of glass with 'strongly' dissimilar materials, i.e. metals or crystals, poses certain challenges, such as extremely different thermal expansion coefficients, but may, in certain cases, relax the necessary constraints imposed on transparent-transparent material joining, e.g. the case for silicon-glass or metal-glass welding where the silicon or metal will always act as a relatively good absorber and therefore, does not require high NA focusing. For instance, USP glass to silicon joining is investigated in [66–69]. USP joining of glass to metals has also been detailed for glass to copper [66, 70–72], glass to aluminum [66, 72, 73], glass to steel [66, 72], glass to sapphire [66] and glass to silicon carbide [74]. There has been a steadily increasing number of publications on USP joining of glass to dissimilar materials, but a thorough explanation of the involved processes, such as formation of mixed glass-metal phases, is unfortunately out of scope for this paper. Nonetheless, from a materialographic viewpoint, the laser-precipitated and mediated interactions of such highly dissimilar materials allow the exploration and understanding of their behavior at extreme conditions (e.g. temperature or pressure) in a tightly localized region. For instance, the extremely high quenching rates achievable during cooldown can be used, in principle, for spatially selective modifications of the glass's conductivity [75].

4.3. Possible applications

The development of the USP glass welding process has been driven by practical applications, such as hermetic sealing, which is critical to the development of many technologies, such as lab-on-chip or MEMS production. One of the early industrial adopters of this process was Glencatec AG, a subsidiary company of mb-microtec AG, where glass encapsulation technology based on USP glass welding was developed for medical implants containing electronic devices accessible via RF [76]. A detailed description of how such an implant can be designed is given in [77], for the use case of blood pressure monitoring. Moreover, system manufacturers targeting these application fields, e.g. LightFab GmbH [78], also implement the USP glass welding process as a tool to expand the range of applications their 3D manufacturing system can cover.

Another application is the encapsulation of optical fibers by fiber end-caps. Reasons for encapsulation vary by application, as fiber end-caps can enlarge the damage threshold of the fiber, or provide hermetic sealing to photonic crystal fibers, thus preventing long-term chemical degradation processes due to the permeation of undesirable outside gases. This type of process has been demonstrated by [79] and used for industrial purposes by Trumpf GmbH [80].

5. Conclusion

Glass welding by ultra-short laser pulses is a piece of technology standing currently on the verge from being an academic research topic to become a key technology for diverse industrial applications. So far, other than the aforementioned applications, USP glass welding was only able to marginally displace the established methods used for glass joining in large-scale industrial applications. This might be due to our current market's low levels of economic competitiveness for the majority of today's applications, in spite of the advantages of USP glass welding. Nonetheless, it can be expected that with decreasing investment costs for USP lasers, as well as relaxations on the preconditions for the specimen to be joined, and joining process as well through further research, it is likely that USP glass welding can one day become an ubiquitous production technology.

Acknowledgments

The authors gratefully acknowledge support by the Graduate School in Advanced Optical Technologies (SAOT) of the Friedrich–Alexander-University of Erlangen–Nürnberg, and the Bayerisches Laserzentrum GmbH.

ORCID iDs

Kristian Cvecek https://orcid.org/0000-0001-7417-4829

References

[1] Petermann K and Voges E 2002 *Optische Kommunikationstechnik* (Berlin: Springer)
[2] Frankel G S, Vienna J D, Lian J, Scully J R, Gin S, Ryan J V, Wang J, Kim S H, Windl W and Du J 2018 *npj Mater. Degrad.* **2** 15

[3] Cailleteau C, Angeli F, Devreux F, Gin S, Jestin J, Jollivet P and Spalla O 2008 *Nat. Mater.* **7** 978
[4] https://heraeus.com/media/media/hca/doc_hca/products_and_solutions_8/optics/Suprasil_UVL_synthetic_fused_silica_EN.pdf
[5] Yaroshevsky A A 2006 *Geochem. Int.* **44** 48
[6] Naumann H and Schröder G 1992 *Optical Construction Elements* (Munich: Hanser Verlag)
[7] Banse H 2005 Laser beam soldering—technology for the setup of optical systems *PhD Thesis* University Jena, Germany
[8] Pleguezuelo P R, Koechlin C, Hornaff M, Kamm A, Beckert E, Fiault G, Eberhardt R and Tünnermann A 2016 *Opt. Eng.* **55** 6
[9] Greco V, Marchesini F and Molesini G 2001 *J. Opt. A: Pure Appl. Opt.* **3** 85
[10] Grünwald F 1985 *Manufacture Processes in Device Engineering* (Munich: Carl Hanser Verlag)
[11] Hecht-Mijic S, Harnisch A, Huelsenberg D, Schundau S, Pfeifer J and Schroeter T 2003 *Mater.wiss. Werkst.tech.* **34** 645
[12] Maruo H, Miyamoto I and Arata Y 1981 CO_2 laser welding of ceramics *1st Int. Laser Processing Conf.* (Laser Institute of America)
[13] Tamaki T, Watanabe W, Nishii J and Itoh K 2005 *Japan. J. Appl. Phys.* **44** 22
[14] Itoh K, Watanabe R and Tamaki T 2005 *Japan Patent* JP002005066629A
[15] Bovatsek J, Arai A Y and Yoshino F 2010 *US Patent Specification* US20100084384
[16] Tamaki T, Watanabe W and Itoh K 2006 *Opt. Express* **14** 22
[17] König J and Bauer T 2011 *Proc. SPIE* **7925** 792510
[18] Kiedrowski T, Michalowski A and Bauer F 2015 *Laser Technik J.* **12** 30
[19] Nolte S, Schrempel F and Dausinger F (ed) 2016 *Ultrashort Pulse Laser Technology* (Cham: Springer) (https://doi.org/10.1007/978-3-319-17659-8)
[20] Miyamoto I, Horn A and Gottmann J 2007 *J. Micro/Nanoeng.* **2** 7
[21] Weber M J 2002 *Handbook of Optical Materials* (Boca Raton, FL : CRC Press) p 261
[22] Topcu T and Robicheaux F 2012 *Phys. Rev.* A **86** 053407
[23] Diels J-C and Rudolph W 2006 *Ultrashort Laser Pulse Phenomena* ed P Liao and P Kelley (Amsterdam: Elsevier) p 205
[24] Senn F, Holtz R, Gross-Barsnick S-M and Reisgen U 2019 *Opt. Express* **27** 27628
[25] Sun M, Eppelt U, Russ S, Hartmann C, Siebert C, Zhu J and Schulz W 2013 *Opt. Express* **21** 7858
[26] Noack J and Vogel A 1999 *IEEE J. Quantum Electron.* **35** 1156
[27] Miyamoto I, Cvecek K, Okamoto Y and Schmidt M 2013 *Appl. Phys.* A **114** 187
[28] Poprawe R 2005 *Lasertechnik für die Fertigung* (Berlin: Springer) p 130
[29] Pfalzner S 2006 *An Introduction to Inertial Confinement Fusion* (London: Taylor and Francis Group) p 73
[30] Cvecek K, Miyamoto I, Heberle J, Bergler M, de L D and Schmidt M 2018 *10th CIRP Conf. on Photonic Technologies (LANE 2018) Proc. CIRP* vol 74, p 339
[31] Vogel A 2009 Roles of tunneling, multiphoton ionization, and cascade ionization for femtosecond optical breakdown in aqueous media (http://dtic.mil/dtic/tr/fulltext/u2/a521817.pdf)
[32] Makabe T and Petrovic Z L 2006 *Plasma Electronics Applications in Microelectronic Device Fabrication* (London: Taylor and Francis Group)
[33] Alexeev I, Heberle J, Cvecek K, Nagulin K Y and Schmidt M 2015 *Micromachines* **6** 1914
[34] Miyamoto I, Okamoto Y, Tanabe R, Ito Y, Cvecek K and Schmidt M 2016 *Opt. Express* **24** 25718
[35] Cvecek K, Miyamoto I, Adam M and Schmidt M 2012 *Phys. Proc.* **39** 563
[36] Davis K M, Miura K, Sugimoto N and Hirao K 1996 *Opt. Lett.* **21** 1729
[37] Gottmann J, Hermans M, Repiev N and Ortmann J 2017 *Micromachines* **8** 110
[38] Cvecek K, Miyamoto I and Schmidt M 2014 *Opt. Express* **22** 15877
[39] Richter S, Döring S, Burmeister F, Zimmermann F, Tünnermann A and Nolte S 2013 *Opt. Express* **21** 15452
[40] Shimizu M, Miura K, Sakakura M, Nishi M, Shimotsuma Y, Kanehira S, Nakaya T and Hirao K 2010 *Appl. Phys.* A **100** 1001
[41] Scholze H 1994 *Glass Nature, Structure and Properties* (Berlin: Springer)
[42] Hashimoto F, Richter S, Nolte S, Ozeki Y and Itoh K 2015 *J. Laser Micro/Nanoeng.* **10** 29
[43] Miyamoto I, Cvecek K and Schmidt M 2013 *Opt. Express* **21** 14291
[44] Cvecek K, Odato R, Dehmel S, Miyamoto I and Schmidt M 2015 *Opt. Express* **23** 5681
[45] http://heraeusquarzglas.de/en/quarzglas/mechanicalproperties/Mechanical_properties.aspx
[46] Cvecek K, Miyamoto I, Strauss J, Wolf M, Frick T and Schmidt M 2011 *Appl. Opt.* **50** 1941
[47] Richter S, Döring S, Tünnermann A and Nolte S 2011 *Appl. Phys.* A **103** 257
[48] Tang Z, Shi T, Liao G and Liu S 2008 *Microelectron Eng.* **85** 1754
[49] Cvecek K, Alexeev I, Miyamoto I and Schmidt M 2010 *Phys. Proc.* **5** 495
[50] Cvecek K, Stenglein F, Miyamoto I and Schmidt M 2017 *J. Laser Micro/Nanoeng.* **12** 115
[51] Lopez J, Mishchik K, Chassagne B, Javaux-Leger C, Hönninger C, Mottay E and Kling R 2015 ICALEO 2015 M404 60 (2015) (https://doi.org/10.2351/1.5063208)
[52] Kennedy P K 1995 *IEEE J. Quantum Electron.* **31** 2241
[53] Shimizu M, Sakakura M, Ohnishi M, Yamaji M, Shimotsuma Y, Hirao K and Miura K 2011 *Opt. Express* **20** 934
[54] Chen J, Carter R M, Thomson R R and Hand D P 2015 *Opt. Express* **23** 18645
[55] Richter S, Zimmermann F, Eberhardt R, Tünnermann A and Nolte S 2015 *Appl. Phys.* A **121** 1–9
[56] Eötvös R 1886 *Ann. der Physik.* **27** 448
[57] Chen H, Deng L, Duan J and Zeng X 2019 *Opt. Lett.* **44** 2570
[58] Blieske U and Stollwerck G 2013 Glass and other encapsulation materials *Semiconductors and Semimetals, Advances in Photovoltaics: Part 2* ed G P Willeke and E R Weber vol 89 (Amsterdam: Elsevier) pp 199–258
[59] Kühn B and Schadrack R 2009 *J. Non-Cryst. Solids* **355** 323
[60] Okamoto Y, Miyamoto I, Cvecek K, Okada A, Takahashi K and Schmidt M 2013 *J. Laser Micro/Nanoeng.* **8** 65
[61] Kongsuwan P, Satoh G and Yao Y L 2012 *J. Manuf. Sci. Eng.* **134** 011004
[62] Miyamoto I, Cvecek K, Okamoto Y, Schmidt M and Helvajian H 2011 *Opt. Express* **19** 22961
[63] Sugioka K, Iida M, Takai H and Midorikawa K 2011 *Opt. Lett.* **36** 2734
[64] Hélie D, Lacroix F and Vallée 2012 *J. Laser Micro/Nanoeng.* **7** 284
[65] Watanabe W, Onda S, Tamaki T, Itoh K and Nishii J 2006 *Appl. Phys. Lett.* **89** 021106
[66] Carter R M, Chen J, Shephard J D, Thomson R R and Hand D P 2014 *Appl. Opt.* **53** 4233

[67] Miyamoto I, Okamoto Y, Hansen A, Vihinen J, Amberla T and Kangastupa J 2015 *Opt. Express* **23** 3427
[68] Horn A, Mingareev I, Werth A, Kachel M and Brenk U 2008 *Appl. Phys.* A **93** 171
[69] Nordin I H W, Okamoto Y, Okada A, Jiang H and Sakagawa T 2016 *Appl. Phys.* A **122** 400
[70] Utsumi A, Ooie T, Yano T and Katsumura M 2007 *J. Laser Micro/Nanoeng.* **2** 133
[71] Ozeki Y, Inoue T, Tamaki T, Yamaguchi H, Onda S, Watanabe W, Sano T, Nishiuchi S, Hirose A and Itoh K 2008 *Appl. Phys. Express* **1** 082601
[72] Zhang G and Cheng G 2015 *Appl. Opt.* **54** 8957
[73] Ciuca O P, Carter R M, Prangnell P B and Hand D P 2016 *Mater. Charact.* **120** 53
[74] Zhang G, Bai J, Zhao W, Zhou K and Cheng G 2017 *Opt. Express* **25** 1702
[75] Hirai K, Tatsumisago M and Minami T 1995 *Solid State Ion.* **78** 269
[77] http://glencatec.com
[77] Kim S, Park J, So S, Ahn S, Choi J, Koo C and Joung Y-H 2019 *Sensors* **19** 1801
[78] https://lightfab.de/
[79] Hélie D, Gouin S and Vallée R 2013 *Opt. Mater. Express* **3** 1742
[80] Kaiser E 2016 *Laser Technik J.* **13** 22